

Effects of Chrysin-PLGA-PEG Nanoparticles on Proliferation and Gene Expression of miRNAs in Gastric Cancer Cell Line

Farideh Mohammadian,¹ Alireza Abhari,² Hassan Dariushnejad,³ Alireza Nikanfar,³ Younes Pilehvar-Soltanahmadi,¹ and Nosratollah Zarghami^{3,*}

¹Department of Medical Biotechnology, Faculty of Advanced Medical Sciences, Tabriz University of Medical Sciences, Tabriz, IR Iran

²Department of Clinical Biochemistry, Faculty of Medicine, Tabriz University of Medical Sciences, Tabriz, IR Iran

³Hematology and Oncology Research Center, Tabriz University of Medical Sciences, Tabriz, IR Iran

*Corresponding author: Nosratollah Zarghami, Hematology and Oncology Research Center, Tabriz University of Medical Sciences, Tabriz, IR Iran. Tel: +98-4133364666, E-mail: zarghami@tbzmed.ac.ir

Received 2015 September 28; Revised 2015 October 26; Accepted 2016 August 10.

Abstract

Background: Recently, Chrysin, as a flavone, has revealed cancer chemo-preventive activity. The present experiment utilized the PLGA-PEG-chrysin complex, and free chrysin, to evaluation of the expression of miR-22, miR-34a and miR-126 in human gastric cell line.

Objectives: The purpose of this study was to examine whether nano encapsulating chrysin improves the anti-cancer effect of free chrysin on AGS human gastric cell line.

Methods: Properties of the chrysin encapsulated in PLGA-PEG nanoparticles were investigated by SEM, H NMR, and FTIR. The assessment of cytotoxicity on the growth of the human gastric cell line was carried out through MTT assay. After treating the cells with a prearranged amount of pure and encapsulated chrysin, RNA was extracted and the expressions of miR-22, miR-34a and miR-126 were measured by using real-time PCR.

Results: With regard to the amount of the chrysin loaded in PLGA-PEG nanoparticles, IC50 value was significantly decreased in nanocapsulated chrysin, in comparison with free chrysin. This finding has been proved through the further increase of miR-22, miR-34a and miR-126 gene expression of nanocapsulated chrysin, in comparison with free chrysin.

Conclusions: In this study, we revealed that the PLGA-PEG-chrysin is more effective than free chrysin in inhibiting the growth of human gastric cell line.

Keywords: Gastric Cancer, Micro RNA, Chrysin, PLGA-PEG, Real-Time PCR

1. Background

Gastric cancer is a major cause of cancer death in Asia and one of the most important causes of cancer-related deaths worldwide (1). Routine protocols are surgery and chemotherapy for gastric cancer treatment. Unfortunately, therapeutic effects of these drugs are not good enough and chemotherapeutic agents have many side effects (2). Recently, many scientists have focused on natural agents that might have therapeutic or protective effects against gastric cancer. In traditional and herbal medicine, numerous flavonoids have been studied to inhibit the development and progress of cancer (3).

Flavonoids are a wide-ranging class of plant pigments that are universally existing in fruit- and vegetable-based foods (4). Flavonoids have been recognized as the main constituent of the human diet which is easily ingested. Excess of 4,000 types of biologically active flavonoids have

been recognized and they can be divided into flavones, flavonols, flavanones, anthocyanidins, and isoflavonoid subclasses (5, 6). One of the naturally wide distributed flavone is Chrysin (5, 7-dihydroxyflavone) which is found in some plants such as passion flowers *Passiflora caerulea*, *Passiflora incarnata*, and in *Oroxylum indicum*. It is, moreover, found in chamomile, *Pleurotus ostreatus*, and honeycomb (7, 8).

It has been proved that chrysin possess anti-inflammatory and anti-oxidant effects, and cancer chemo-preventive activity through induction of apoptosis process in various human and rat cell lines. However, reports of the results of chrysin effectiveness on human cancers remain scarce (9, 10).

The low water solubility of chrysin limits their bioavailability and biomedical applications. To overcome this problem, various approaches can be used (11, 12). The use

of nanoparticles is one of the ways to achieve this goal (13, 14).

One of the most exciting delivery services for transferring different anticancer therapeutic agents are the nanoparticles which are self-assembled from amphiphilic polymers (15, 16). The polymeric nanoparticles form the core-shell organization by self-assembly in aqueous medium. The hydrophobic core (inner layer) holds the anticancer drugs and the hydrophilic shell (the outer layer) stabilizes the nanoparticles. The drug-loaded polymeric nanoparticles have improved pharmacological structures for the accumulation in tumor tissue or cells because of the improved retention (EPR) effect and penetrability, which can improve drug tolerance and reduce adverse effects (17, 18).

Poly(lactic-co-glycolic acid) (PLGA) is one of biodegradable polymer nanoparticles approved by FDA because of its hydrolyzation to natural monomeric metabolites, glycolic acid and lactic acid (19-21). So, the encapsulation of anticancer drugs such as chrysin in biodegradable PLGA nanoparticles may offer many advantages over other delivery system.

MicroRNAs (miRNA) with 20 to 23 nucleotides length are endogenous small noncoding RNAs that are involved in control of gene expression posttranscriptional and play important roles in carcinogenesis and human gastric cancer progress (22).

2. Objectives

This study investigates the anti-proliferative effects of chrysin and compares them with PLGA-PEG-chrysin complex on cancer related micro RNA expression, including miR-22, miR-34a, and miR-126.

3. Methods

3.1. Chemical and Reagents

RPMI 1640, fetal bovine serum (FBS), Trypsin- EDTA and antibiotics were purchased from Invitrogen (Germany). PLGA-PEG, 3- (4, 5-Dimethylthiazol-2-yl)-2, 5-diphenyltetrazolium bromide (MTT), and chrysin were purchased from Sigma (USA). Syber green real time PCR master mix kit was purchased from Exiqon (Denmark). Dimethyl sulphoxide (DMSO), Stannous octoate (Sn (Oct) 2: stannous 2-ethylhexanoate), D, L-lactide and glycolide and polyethylene glycol (PEG) were purchased from Sigma (St Louis, USA).

3.2. Cell Culture and Cell Line

AGS human gastric cell line was provided by Pasteur institute cell bank of Iran. AGS human gastric cell line were cultured in RPMI 1640 complemented with 0.08 mg/mL streptomycin, 0.05 mg/mL penicillin G, 2 mg/mL sodium bicarbonate, 10% heat-inactivated fetal bovine serum (FBS), and cells were grown at 37°C in an incubator with 55% humidity and 5% CO₂.

3.3. Synthesis of PLGA-PEG

PLGA-PEG was prepared through ring open polymerization of glycolide and DL lactide followed by addition of PEG under vacuum. PLGA and PEG were co-polymerized in presence of stannous octoate as the catalyst. Under a nitrogen atmosphere, DL-lactide (2.882g), glycolide (0.570 g) and PEG6000 1.54 g (45% w/w) were melted in bottleneck flask in 140 Celsius degrees. Reaction mixture comprising a 1; 3 proportion of glycolide to DL-lactide and 0.05% (w/w) stannous octoate was obtained and heated up to 180°C and sustained for 4 hours.

3.4. Preparation of Chrysin-Loaded PLGA-PEG

Chrysin were encapsulated in PLGA-PEG nanoparticle by using w/o/w technique. Briefly, PLGA-PEG (200 mg) and pure chrysin (20 mg) were dissolved in dichloromethane (DCM) and sonicated for 1 minute to allow chrysin to be entrapped within the nanoparticle network (the w/o primary mixture). Polyvinyl alcohol (PVA) and DMSO 1% (1: 1) were added to w/o emulsion then sonicated for 1 minute to produce w/o/w emulsion. Then, dichloromethane was evaporated using a rotary evaporator and the remaining solution was centrifuged at 10000 rpm for 30 minutes.

The supernatant was isolated and compared with the total amount of chrysin to determine the chrysin loading efficiency of the nanoparticles. The amount of non-entrapped chrysin in aqueous phase was determined using an ultraviolet 2550 (lambda max 348 nm) spectrophotometer (Shi-madzu). The percent of chrysin encapsulated on the nanoparticles (EE) (Equation 1) and drug loading (DL) (Equation 2) was measured using the following formula:

$$EE = \frac{\text{Weight of CHRYSIN in NP}}{\text{Weight of the initial drug}} \times 100 \quad (1)$$

$$DL = \frac{\text{Weight of CHRYSIN in NPs}}{\text{Weight of NPs}} \times 100 \quad (2)$$

This procedure permits the analysis of a chrysin solution with the removal of most interfering substances.

SEM was applied as determination of size and shape of chrysin and chrysin-PLGA-PEG nanoparticles. The FTIR spectrum was achieved from a neat film cast of the chloroform copolymer solution between KBr tablets. The ¹H NMR spectra were traced in CDCl₃ (23, 24).

3.5. Cell Viability and MTT-Based Cytotoxicity Assay

After culturing a sufficient amount of cells (exponential phase of growth), the cytotoxic effects of pure and PLGA-PEG-loaded chrysin on AGS cell line were studied using 24-hour, 48-hour, and 72-hour MTT assays. In brief, 10000 cells/well were cultivated in a 96-well plate (Nunc, Denmark) and kept for 24 hours in the incubator at 37°C in a humidified atmosphere including 5% CO₂ to promote cell attachment. Then, the cells were treated with serial concentrations of pure and PLGA-PEG-loaded Chrysin (0 - 160 μM) for 24, 48, and 72 hours in triplicate manner. As a control, cells received 200 μL culture medium containing 10% dimethyl sulfoxide. After this exposure time, the old medium in all wells of the 96-well plate was replaced with 200 μL fresh medium and the cells were held for 24 hours in an incubator at 37°C. The medium in all the wells was then eliminated carefully, and 50 μL of 2 mg/mL MTT dissolved in phosphate-buffered solution (PBS) was added to each well. The plate was covered with aluminum foil and incubated for 4 hours in an incubator at 37°C. Then, 200 μL of pure DMSO and 25 μL of Sorensen's glycine buffer was added to the all wells after slowly eliminating the contents of the wells. Next, the absorbance of each well was read and record at 570 nm using an EL X 800 microplate absorbance reader (Bio Tek Instruments, Winooski, VT) with a reference wavelength of 630 nm.

3.6. RNA Extraction, cDNA Synthesis and Real Time PCR

Expression of miR-22, miR-34a and miR-126 were assessed by qRT-PCR. Triplicate assays were performed for each RNA sample. AGS human gastric cell line were treated with different concentrations of PLGA-PEG-Chrysin and pure chrysin (25, 35, 55 and 70 μM) for 24 hours in order to extract RNA. Total RNA was isolated using Exiqon miR-CURY RNA isolation kit (Exiqon, Denmark) according to the manufacturer instructions. A spectrophotometer was applied to ensure the purity of the extracted RNA, and it was measured at a wavelength of 260 - 280 nm. CDNA synthesis was done according to LNA universal RT miRNA PCR kit (Exiqon, Denmark). CDNA was amplified with particular primers of the miR-22, miR-34a and miR-126 genes and the internal control gene (miR-16). SyberGreen qPCR Mix purchased from Exiqon (denmark) and used for real time PCR. Real time PCR was done using Corbett 6000. Mir-16 was used as the endogenous control miRNA.

3.7. Statistical Analysis

Statistical analysis was performed using GraphPad.Prism.6.01 and the ANOVA test (by one-way analysis of variance) to measure statistical differences among groups. Data with P-value smaller than 0.05 were considered to be statistically significant.

4. Results

4.1. ¹H NMR Spectrum of PEG-PLGA Copolymer

¹H NMR spectra confirmed the basic chemical structure of the PEG-PLGA copolymer. The chemical shifts were measured in ppm using tetramethylsilane (TMS) as an internal reference. One of the striking features is a large peak at 3.7 ppm, corresponding to the methylene groups of the PEG. Overlapping bands at 1.6 ppm are assigned to the methyl groups of the repeating units of L-lactic acid and D-lactic acid. The multiple peaks at 4.8 and 5.3 ppm assigned to the glycolic acid CH and the lactic acid CH respectively (Figure 1).

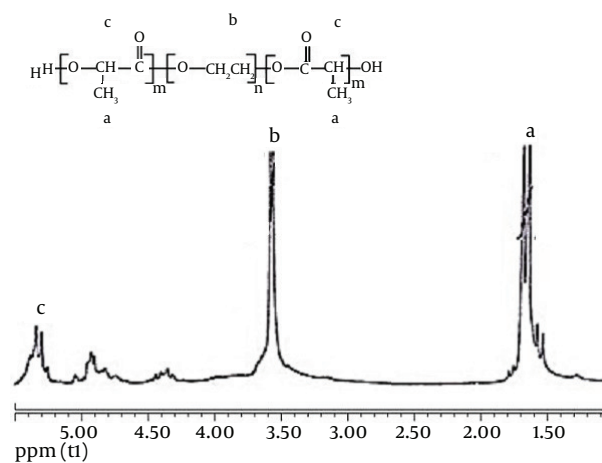


Figure 1. ¹H NMR Spectrum of PEG-PLGA co-Polymer

4.2. FT-IR Spectroscopy

The FT-IR spectrum is in harmony with the structure of the anticipated copolymer. FT-IR spectroscopy was prepared to illustrate the structure of PLGA-PEG copolymer nanoparticles with chrysin. As shown in Figure 2B, the absorption band at 3000 - 2840 cm⁻¹ and 3509.9 cm⁻¹ are due to C-H stretch of CH and the terminal hydroxyl groups in the copolymer (respectively). The bands at 1300-1090 cm⁻¹ are assigned to interaction between C-C and C-O. Some chemical shifts accrued in FT-IR spectra after encapsulation. As shown in Figure 2, the bands at 1085 - 1150 cm⁻¹ are assigned to either of PEG. The bands at 1090 - 1300 cm⁻¹ are due to interaction between C-O and C-C. The bands at 2840 - 3000 cm⁻¹ are due to C-H stretch of CH.

All the ¹H-NMR and FT-IR results indicated that the PLGA-PEG copolymer formed successfully and chrysin loaded into PLGA-PEG.

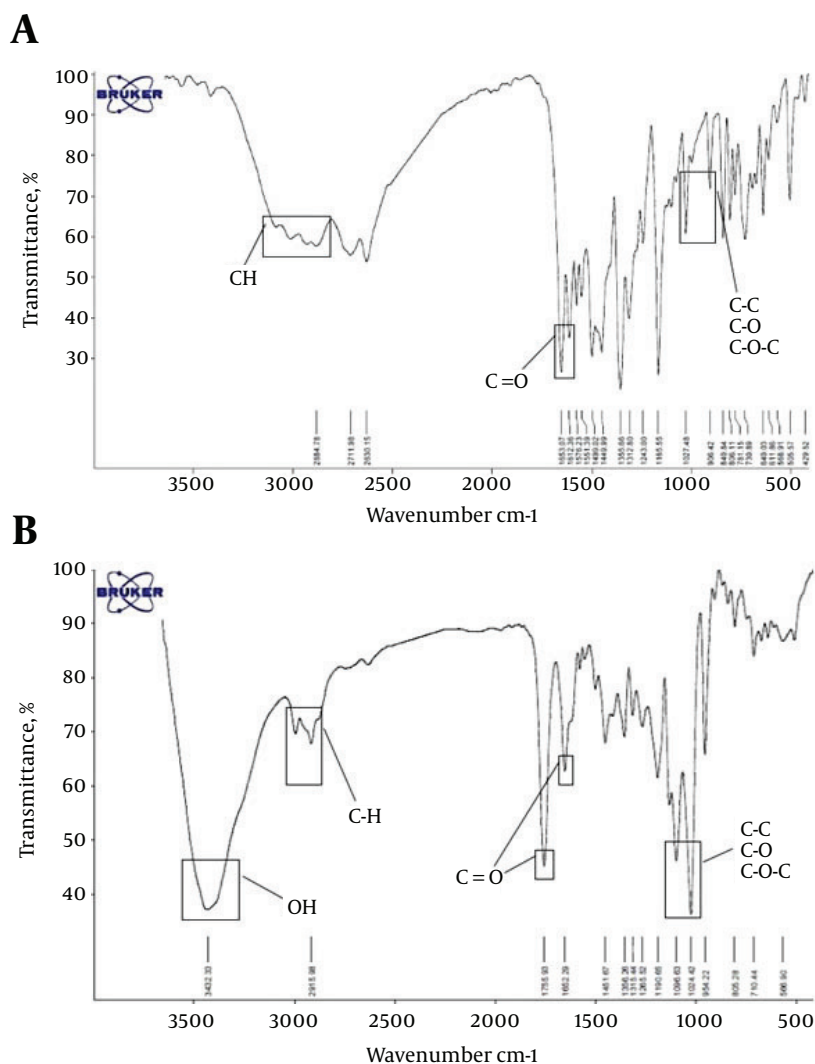


Figure 2. A, IR spectrum of pure chrysin; B, FT-IR plot of chrysin loaded PLGA-PEG

4.3. Size and Size Distribution (Scanning Election Microscopy)

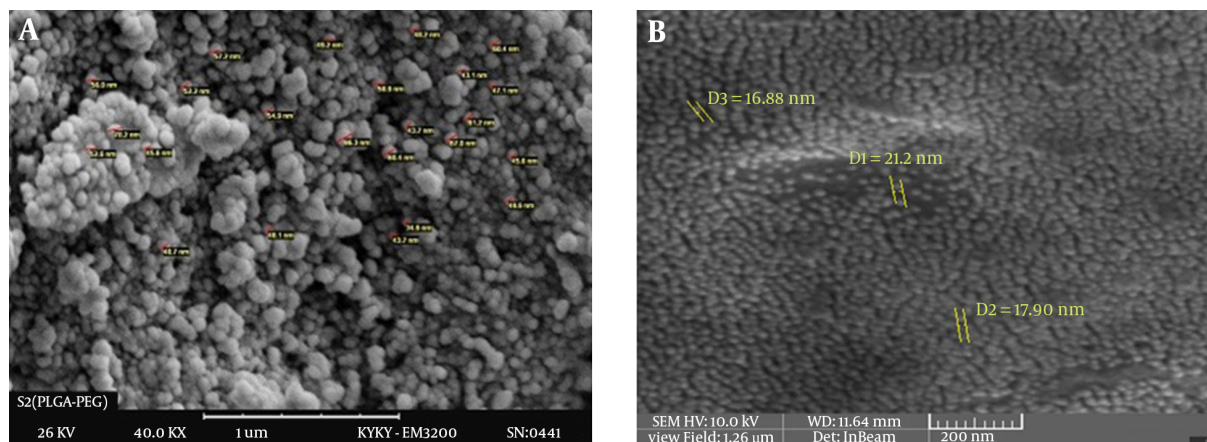
In order to investigate the physicochemical characterization of nanoparticles, the nanoparticles were observed by scanning electron microscopy (SEM) (Figure 3). It was observed from these micrographs that the nanoparticles of PLGA-PEG were spherical in shape and uniform, with the size ranging from 15 - 60 nm (Figure 3A). The photograph shows that after encapsulation and the formation of chrysin-loaded PLGA-PEG copolymers, the size of the particles was changed, and ranged between 20 - 75 nm, and the dispersion of particles was greatly improved (Figure 3B).

4.4. Entrapment Efficiency (EE) and Drug Loading (DL)

According to Equation 1 Encapsulation efficiency (EE) and drug loading (DL) of chrysin in PLGA-PEG was 94.6% and 16.19%, respectively.

4.5. In Vitro Cytotoxicity Study (MIT Assay)

In the cytotoxicity assay, AGS cell lines were treated with free chrysin and increasing concentration of PLGA-PEG-chrysin (0 - 160 μM) for 24, 48 and 72 hours. Then, the value of inhibitory concentration 50 (IC50) was calculated for each case. Significant differences in the growth pattern were found between control and cells treated with free chrysin or PLGA-PEG-chrysin. The IC50 value of free chrysin was 68.24 μM for 24 hours, 56.16 μM for 48 hours

Figure 3. Chrysin and Nano Chrysin in Scanning Electron Microscopy Micrograph

A, The size of PLGA-PEG and; b, drug loaded in PLGA-PEG nanoparticle.

and 42.32 μM for 72 hours. The IC₅₀ value of PLGA-PEG-chrysin was 58.24 μM for 24 hours, 44.21 μM for 48 hours and 36.8 μM for 72 hours (Figure 4).

4.6. Expression Level of miR-22, miR-34a and miR-126

Quantitative gene expression for miR-22, miR-34a and miR-126 was examined by real-time PCR assay in the AGS cell lines after treatment with free chrysin and PLGA-PEG-chrysin, and compared with controls. The relative levels of microRNA gene expression were calculated through the $\Delta\Delta\text{CT}$ method. With regard to the data analysis shown in Figure 5, free and encapsulated chrysin, with a concentration of (25, 35, 55 and 70 μM) after 24 hours, showed significantly increased gene expression. Whereas chrysin loaded in PLGA-PEG nanoparticle in same concentration increased further relative mRNA expression of miR-22, miR-34a and miR-126 (Figure 5A - 5C).

5. Discussion

The mortality associated with Human gastric cancer is still a major problem worldwide (25). However, conventional treatment strategies for gastric cancer are not yet adequate.

The objective of the present study was to evaluate the effect of chrysin-PLGA-PEG on general miRNAs (miR-22, miR-34a and miR-126) expression for gastric cancer in AGS cell line.

Recently, studies have shown that a change of miRNA expression (increase or decrease) contributes to the initiation and progression of cancer. It has been shown that more than 50% of miRNAs are located in fragile sites or in

cancer associated genomic regions (26). The relationship between tumors and miRNA has at this time become the heart of cancer studies.

Although various methods such as chemotherapy, gene therapy and hormone therapy are studied and used for treating cancer (27), the most recently popular method is the use of polymer nanoparticles for the delivery of anti-cancer drugs to cancer tissue. This is more efficient than using free drugs, and owing to the use of low dose of drug, the toxicity is decreased.

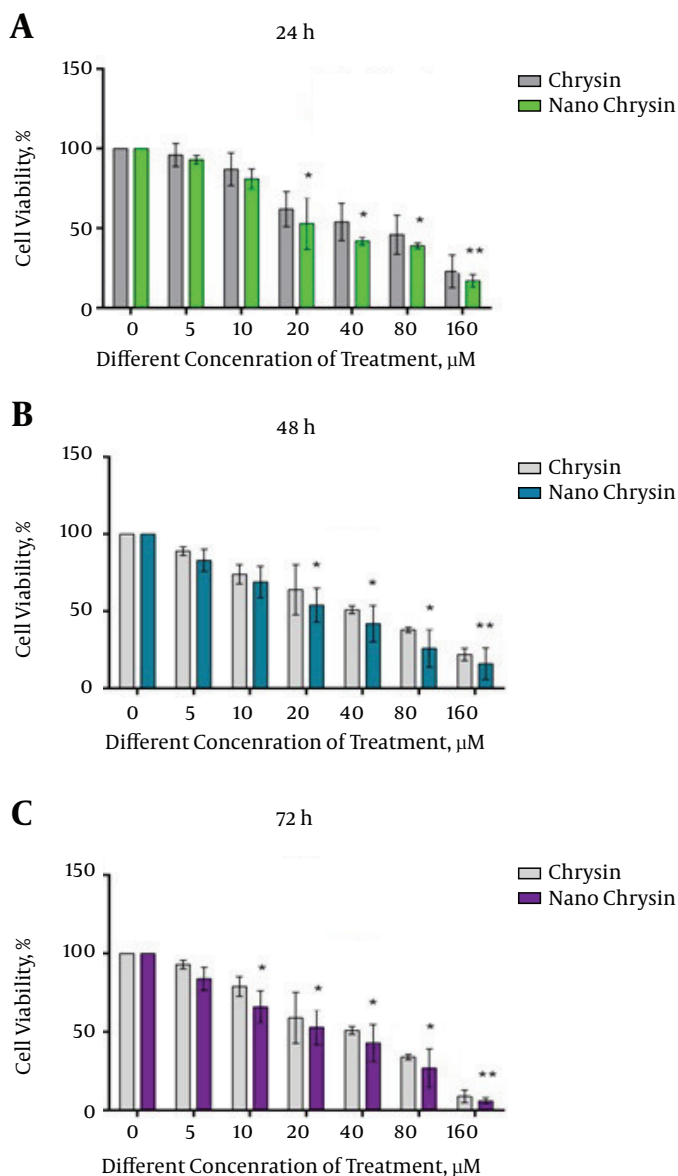
The data obtained from MTT analysis indicates that IC₅₀ of free chrysin and PLGA-PEG encapsulated chrysin in the AGS cell line is both dose dependent and time-dependent but the result improves with nanocapsulation form of chrysin.

MiRNAs can be classified as tumor suppressors or as oncogenes by targeting different transcripts. Mir-22, mir-34a and mir-126 play as tumor suppressors in gastric cancer and down-regulated in gastric cancer tissue (28).

Guo et al. showed that SP1 was one of the target genes for miR-22. SP1 is recognized as a transcriptional factor for various genes regulated cellular process and also participates in cancer progression and development (Sp1 and the 'hallmarks of cancer'). In this study we found that chrysin increase miR-22 expression level and it can be concluded that chrysin can inhibit gastric cancer cell migration and invasion through the SP1 pathway (29).

Down regulation of mir-34a inhibits apoptosis in gastric cancer and it is proved that miR-34 is involved the P53 tumor suppressor network. Chrysin increased miR-34 expression in our study. Restoration of miR-34 activity may be useful to prevent chemoresistance an able to reestablish

Figure 4. Comparison of Cytotoxic Effects for Different Concentration of Pure and Nano Chrysin for 24, 48 and 72 Hours



A, B and C related to treatment for 24, 48 and 72 hours, respectively. Results expressed as the mean \pm SEM (n = 3), (*P < 0.05, **P < 0.01).

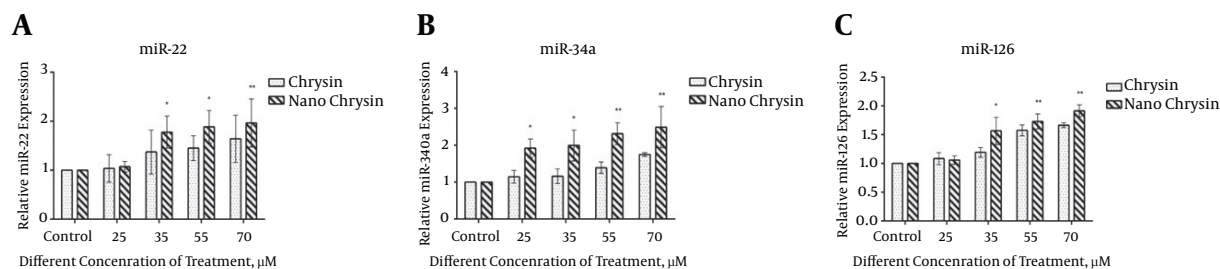
the tumor suppressing signaling pathway (30).

MiR-126 functions as a tumor suppressor in gastric cancer. MiR-126 down regulates in this cancer and targets Crk. Crk plays an important role in cancer development and metastasis. Our results show that chrysin elevates the amount of miR-126 in AGS cell line (31).

The assessment of miR-22, miR-34a and miR-126 gene expression by real time PCR showed that miRNAs expression increased on exposure to both free chrysin and PLGA-

PEG encapsulated chrysin, whereas nancapsulated form of chrysin increased expression of miRNAs more than pure chrysin.

This study showed that chrysin has a significant inhibitory effect on the growth of AGS human gastric cell line. Using polymer nanoparticles, the dose of chrysin administered could be reduced, without reducing its therapeutic efficiency and effect. Therefore, PLGA-PEG encapsulated chrysin preserved its full function. In addition,

Figure 5. (A), (B) and (C) Shows Comparison Between Effect of Chrysin and Nano-Chrysin on miR-22, miR-34a and miR-126 Expression Respectively

Result shows that nanocapsulated form of chrysin are more effective to increase the expression level of micro RNAs. Data are presented as mean \pm SEM from three independent experiments, (*P < 0.05, **P < 0.01).

chrysin may be useful for increasing restoration of tumor suppressor miRNA expression levels.

Acknowledgments

Authors would like to thank hematology and oncology research center, Tabriz University of Medical Sciences for supporting this project (grant No: 92/34).

Footnotes

Authors' Contribution: None declared.

Conflict of Interests: The authors declare that they have no conflict of interest.

Financial Disclosure: None declared.

Funding/Support: None declared.

References

- Hundahl SA, Phillips JL, Menck HR. The National Cancer Data Base Report on poor survival of U.S. gastric carcinoma patients treated with gastrectomy: Fifth Edition American Joint Committee on Cancer staging, proximal disease, and the "different disease" hypothesis. *Cancer*. 2000;**88**(4):921-32. [PubMed: 10679663].
- Treasure T, Fallowfield L, Lees B, Farewell V. Pulmonary metastasectomy in colorectal cancer: the PulMiCC trial. *Thorax*. 2012;**67**(2):185-7. doi: 10.1136/thoraxjnl-2011-200015. [PubMed: 21561890].
- Cragg L, Fox A, Nation K, Reid C, Anderson M. Neural correlates of successful and partial inhibitions in children: an ERP study. *Dev Psychobiol*. 2009;**51**(7):533-43. doi: 10.1002/dev.20391. [PubMed: 19685486].
- Robards K, Antolovich M. Analytical chemistry of fruit bioflavonoids: A review. *Analyst*. 1997;**122**(2):11-34.
- Kale A, Gawande S, Kotwal S. Cancer phytotherapeutics: role for flavonoids at the cellular level. *Phytother Res*. 2008;**22**(5):567-77. doi: 10.1002/ptr.2283. [PubMed: 18398903].
- Nijveldt RJ, van Nood E, van Hoorn DE, Boelens PG, van Norren K, van Leeuwen PA. Flavonoids: a review of probable mechanisms of action and potential applications. *Am J Clin Nutr*. 2001;**74**(4):418-25. [PubMed: 11566638].
- Anandhi R, Annadurai T, Anitha TS, Muralidharan AR, Najmunnisha K, Nachiappan V, et al. Antihypercholesterolemic and antioxidative effects of an extract of the oyster mushroom, *Pleurotus ostreatus*, and its major constituent, chrysin, in Triton WR-1339-induced hypercholesterolemic rats. *J Physiol Biochem*. 2013;**69**(2):313-23. doi: 10.1007/s13105-012-0215-6. [PubMed: 23104078].
- Brown E, Hurd NS, McCall S, Ceremuga TE. Evaluation of the anxiolytic effects of chrysin, a *Passiflora incarnata* extract, in the laboratory rat. *AANA J*. 2007;**75**(5):333-7. [PubMed: 17966676].
- Cho H, Yun CW, Park WK, Kong JY, Kim KS, Park Y, et al. Modulation of the activity of pro-inflammatory enzymes, COX-2 and iNOS, by chrysin derivatives. *Pharmacol Res*. 2004;**49**(1):37-43. [PubMed: 14597150].
- Woodman OL, Chan E. Vascular and anti-oxidant actions of flavonols and flavones. *Clin Exp Pharmacol Physiol*. 2004;**31**(11):786-90. doi: 10.1111/j.1440-1681.2004.04072.x. [PubMed: 15566394].
- Eatemadi A, Daraee H, Zarghami N, Melat Yar H, Akbarzadeh A. Nanofiber: Synthesis and biomedical applications. *Artif Cells Nanomed Biotechnol*. 2016;**44**(1):11-21. doi: 10.3109/21691401.2014.922568. [PubMed: 24905339].
- Eatemadi A, Daraee H, Karimkhanloo H, Kouhi M, Zarghami N, Akbarzadeh A, et al. Carbon nanotubes: properties, synthesis, purification, and medical applications. *Nanoscale Res Lett*. 2014;**9**(1):393. doi: 10.1186/1556-276X-9-393. [PubMed: 25170330].
- Daraee H, Eatemadi A, Abbasi E, Fekri Aval S, Kouhi M, Akbarzadeh A. Application of gold nanoparticles in biomedical and drug delivery. *Artif Cells Nanomed Biotechnol*. 2016;**44**(1):410-22. doi: 10.3109/21691401.2014.955107. [PubMed: 25229833].
- Daraee H, Eatemadi A, Kouhi M, Alimirzalu S, Akbarzadeh A. Application of liposomes in medicine and drug delivery. *Artif Cells Nanomed Biotechnol*. 2016;**44**(1):381-91. doi: 10.3109/21691401.2014.953633. [PubMed: 25222036].
- Bae Y, Kataoka K. Intelligent polymeric micelles from functional poly(ethylene glycol)-poly(amino acid) block copolymers. *Adv Drug Deliv Rev*. 2009;**61**(10):768-84. doi: 10.1016/j.addr.2009.04.016. [PubMed: 19422866].
- Chen W, Zhong P, Meng F, Cheng R, Deng C, Feijen J, et al. Redox and pH-responsive degradable micelles for dually activated intracellular anticancer drug release. *J Control Release*. 2013;**169**(3):171-9. doi: 10.1016/j.jconrel.2013.01.001. [PubMed: 23306022].
- Lai Y, Long Y, Lei Y, Deng X, He B, Sheng M, et al. A novel micelle of coumarin derivative monoend-functionalized PEG for anti-tumor drug delivery: in vitro and in vivo study. *J Drug Target*. 2012;**20**(3):246-54. doi: 10.3109/1061186X.2011.639023. [PubMed: 22118403].
- Akbarzadeh A, Samiei M, Joo SW, Anzaby M, Hanifepour Y, Nasrabadi HT, et al. Synthesis, characterization and in vitro studies of doxorubicin-loaded magnetic nanoparticles grafted to smart copolymers on A549 lung cancer cell line. *J Nanobiotechnology*. 2012;**10**:46. doi: 10.1186/1477-3155-10-46. [PubMed: 23244711].

19. Eatemadi A, Darabi M, Afraidooni L, Zarghami N, Daraee H, Eskandari L, et al. Comparison, synthesis and evaluation of anticancer drug-loaded polymeric nanoparticles on breast cancer cell lines. *Artif Cells Nanomed Biotechnol.* 2016;**44**(3):1008-17. doi: [10.3109/21691401.2015.1008510](https://doi.org/10.3109/21691401.2015.1008510). [PubMed: [25707442](https://pubmed.ncbi.nlm.nih.gov/25707442/)].
20. Ghalhar MG, Akbarzadeh A, Rahmati M, Mellatyar H, Dariushnejad H, Zarghami N, et al. Comparison of inhibitory effects of 17-AAG nanoparticles and free 17-AAG on HSP90 gene expression in breast cancer. *Asian Pac J Cancer Prev.* 2014;**15**(17):7113-8. [PubMed: [25227799](https://pubmed.ncbi.nlm.nih.gov/25227799/)].
21. Seidi K, Eatemadi A, Mansoori B, Jahanban-Esfahlan R, Farajzadeh D. Nanomagnet-based detoxifying machine: an alternative/complementary approach in HIV therapy. *J AIDS Clinic Res.* 2014;**2014**.
22. Guo J, Miao Y, Xiao B, Huan R, Jiang Z, Meng D, et al. Differential expression of microRNA species in human gastric cancer versus non-tumorous tissues. *J Gastroenterol Hepatol.* 2009;**24**(4):652-7. doi: [10.1111/j.1440-1746.2008.05666.x](https://doi.org/10.1111/j.1440-1746.2008.05666.x). [PubMed: [19175831](https://pubmed.ncbi.nlm.nih.gov/19175831/)].
23. Nabid MR, Bide Y. H40-PCL-PEG unimolecular micelles both as anchoring sites for palladium nanoparticles and micellar catalyst for Heck reaction in water. *Applied Catalysis.* 2014;**469**:183-90.
24. Xia W, Chang J, Lin J, Zhu J. The pH-controlled dual-drug release from mesoporous bioactive glass/polypeptide graft copolymer nanomicelle composites. *Eur J Pharm Biopharm.* 2008;**69**(2):546-52. doi: [10.1016/j.ejpb.2007.11.018](https://doi.org/10.1016/j.ejpb.2007.11.018). [PubMed: [18248801](https://pubmed.ncbi.nlm.nih.gov/18248801/)].
25. Tan YK, Fielding JW. Early diagnosis of early gastric cancer. *Eur J Gastroenterol Hepatol.* 2006;**18**(8):821-9. [PubMed: [16825897](https://pubmed.ncbi.nlm.nih.gov/16825897/)].
26. Calin GA, Sevignani C, Dumitru CD, Hyslop T, Noch E, Yendamuri S, et al. Human microRNA genes are frequently located at fragile sites and genomic regions involved in cancers. *Proc Natl Acad Sci U S A.* 2004;**101**(9):2999-3004. doi: [10.1073/pnas.0307323101](https://doi.org/10.1073/pnas.0307323101). [PubMed: [14973191](https://pubmed.ncbi.nlm.nih.gov/14973191/)].
27. Kennedy S, Geradts J, Bydlon T, Brown JQ, Gallagher J, Junker M, et al. Optical breast cancer margin assessment: an observational study of the effects of tissue heterogeneity on optical contrast. *Breast Cancer Res.* 2010;**12**(6):91. doi: [10.1186/bcr2770](https://doi.org/10.1186/bcr2770). [PubMed: [21054873](https://pubmed.ncbi.nlm.nih.gov/21054873/)].
28. Yao Y, Suo AL, Li ZF, Liu LY, Tian T, Ni L, et al. MicroRNA profiling of human gastric cancer. *Mol Med Rep.* 2009;**2**(6):963-70. doi: [10.3892/mmr_00000199](https://doi.org/10.3892/mmr_00000199). [PubMed: [21475928](https://pubmed.ncbi.nlm.nih.gov/21475928/)].
29. Guo MM, Hu LH, Wang YQ, Chen P, Huang JG, Lu N, et al. miR-22 is down-regulated in gastric cancer, and its overexpression inhibits cell migration and invasion via targeting transcription factor Sp1. *Med Oncol.* 2013;**30**(2):542. doi: [10.1007/s12032-013-0542-7](https://doi.org/10.1007/s12032-013-0542-7). [PubMed: [23529765](https://pubmed.ncbi.nlm.nih.gov/23529765/)].
30. Hermeking H. The miR-34 family in cancer and apoptosis. *Cell Death Differ.* 2010;**17**(2):193-9. doi: [10.1038/cdd.2009.56](https://doi.org/10.1038/cdd.2009.56). [PubMed: [19461653](https://pubmed.ncbi.nlm.nih.gov/19461653/)].
31. Feng R, Chen X, Yu Y, Su L, Yu B, Li J, et al. miR-126 functions as a tumour suppressor in human gastric cancer. *Cancer Lett.* 2010;**298**(1):50-63. doi: [10.1016/j.canlet.2010.06.004](https://doi.org/10.1016/j.canlet.2010.06.004). [PubMed: [20619534](https://pubmed.ncbi.nlm.nih.gov/20619534/)].